ELSEVIER

Journal of Alloys and Compounds 235 (1996) 41–47

Journal of ALLOYS AND COMPOUNDS

Synthesis and crystal structure of nitrate enclathrated sodalite $Na_8[AlSiO_4]_6(NO_3)_2$

Josef-Christian Buhl[a], Jürgen Löns[b]

[a]*Institut für Mineralogie, Universität Hannover, Welfengarten 1, D-30167 Hannover, Germany*
[b]*Institut für Mineralogie, Universität Münster, Correnssstr. 24, D-48149 Münster, Germany*

Received 17 October 1995; in final form 31 October 1995

Abstract

The hydrothermal formation of sodalites in the system Na_2O–$2SiO_2$–Al_2O_3–$NaNO_3$–H_2O has been investigated. Besides temperature and pressure, the initial materials of synthesis were varied to obtain the most perfect single crystals of nitrate enclathrated in sodalite. The alkaline transformation of Zeolite A as the starting aluminosilicate at a temperature of 648 K and a pressure of 0.1 GPa has been proved to be the best method for sodalite synthesis.

A single crystal structure refinement, as well as MAS NMR of the nucleus ^{23}Na of nitrate sodalite, have been carried out to determine the position of the enclathrated nitrate anions in the open sodalite structure. The nitrogen atoms are located in an off-centre position within the sodalite cages. One of the three oxygen atoms of the nitrate group is positioned near the centre of a face of the tetrahedron formed by the sodium cations. The two remaining oxygen atoms of the nitrate group are located near the middle of the edges of the sodium tetrahedron. This arrangement of the nitrate anions is responsible for two split-positions of the sodium cations according to an occupancy ratio of 3:1.

Keywords: Hydrothermal synthesis; Nitrate sodalite; Enclathration compounds; MAS NMR; Structure refinement

1. Introduction

Thorough investigations of several sodalite compounds have demonstrated the model character of these tectosilicates as 'reservoir minerals' according to their large variety of chemical compositions produced by cation exchange, substitution of framework atoms or formation of various solid solutions [1–7]. The enclathration of hazardous components from waste materials seems to be a versatile tool for both material science and waste management [8–11].

We continue these investigations on the incorporation of several oxoanions into the sodalite matrix by studying the sodalite–nitrate interaction. The intercalation of nitrates into porous tectosilicates is of great importance for future applications, because nitrate is a common hazardous component in the environment and is responsible for water pollution. Our recent investigations gave evidence of the formation of nitrite–nitrate sodalite solid solutions [12], but also showed a possibility for pure nitrate intercalation into the β-cages of the sodalite structure [13]. Whereas the nitrate sodalites described first were very imperfect and their crystals always tended to be twinned, we were now able to extend these studies in the areas of both synthesis and structure determination.

2. Experimental

2.1. Synthesis

The system Na_2O–$2SiO_2$–Al_2O_3–$NaNO_3$–H_2O has been investigated under hydrothermal conditions in the 353–773 K temperature interval. Syntheses were carried out under high temperatures and pressures (573–773 K and 0.1–0.15 GPa) in 18 ml steel autoclaves, using silver liners (80 mm length; 8 mm diameter) as sample containers. These liners were filled with 50 mg Kaolin (Fluka 60609) sintered at 1673 K, or 50 mg Zeolite A (Fluka 69836) or 50 mg of a 2:1 mixture of SiO_2 (Merck 657) and γ-Al_2O_3 (Merck 1095) sintered for 2 h at 1673 K. 300 mg of $NaNO_3$ (Merck 6537) were added together with 1 ml 8 M

SSDI 0925-8388(95)02148-5

NaOH (Merck 6495) in every case. The autoclaves were heated in a special vertical cylinder furnace. A pressure up to 0.15 GPa, estimated from the Kennedy diagram, was controlled by the degree of filling.

Teflon® coated steel autoclaves of 50 ml interior volume were used for the experiments at low temperatures and pressures (353–473 K; autogenous pressure up to 0.01 GPa). The Teflon® liners were filled with 1.0 g of the aluminosilicate educts, mentioned above, together with 4.0 g of sodium nitrate and 45 ml 8 M solution of sodium hydroxide.

After a reaction period of 48 h the products were washed with distilled water and dried at 353 K. The various synthesis parameters are summarized in Tables 1(a) and 1(b).

2.2. Characterization

The products were analysed by X-ray powder diffraction, using a Guinier–Jagodzinski camera (Cu $K\alpha_1$ radiation, internal Si-standard). The cell parameters were calculated by least squares refinement.

Those species which can be incorporated into the sodalite cages during crystal growth, i.e. nitrate, water molecules, hydroxyl groups, as well as impurities of carbonate from the mother liquor, were distinguished by means of IR spectroscopy using a Perkin–Elmer spectrometer 683 (KBr pellets) [14,15]. The degree of filling of the sodalite cages with the guest species has been checked by thermogravimetry in connection with IR spectroscopy and X-ray diffraction.

A dodecahedral-shaped crystal of average dimensions of 0.10 mm was selected for structure refinement. Precession photographs showed reflections consistent with space group symmetry $P\bar{4}3n$ [16]. The Enraf–Nonius four circle diffractometer CAD 4 was used for the data collection (Mo $K\alpha$ radiation, graphite monochromator). 8805 independent reflections were collected up to a 2Θ maximum of 120° ($\Theta/2\Theta$ scan mode). Lorentz polarization and spherical absorption correction were applied to the measured data. 42 free structural parameters were varied, including an overall scale factor as well as an isotropic extinction parameter. Further details of the data collection and reduction procedure are summarized in Table 2.

The program SHELX [17] was used for structure refinement. The atomic scattering factors for neutral atoms were taken from Ref. [16], whereas the initial positional parameters were chosen from the single crystal refinement of sodium nitrite sodalite [18]. For an accurate determination of the position of the intercalated guest anions, constraints for the bonding distances and angles of the nitrate group were applied, considering the NO_3^- as a rigid body with regular geometry, as found in solid $NaNO_3$ [19,20]. Therefore, the real position of the guest anions inside the sodalite cages could be revealed.

Besides X-ray diffraction results, additional structural data could be estimated via MAS NMR of the ^{23}Na nucleus, performed on a Bruker MSL-400 FT-NMR spectrometer. The spectra were recorded at 105.8 MHz with 1.7 μs excitation pulses of 70 kHz am-

Table 1
Conditions of the hydrothermal syntheses together with the reaction products obtained

Expt. No.	Initial substance	Temperature (K)	Pressure (GPa)	Reaction products[a]
(a) Low temperature syntheses at autogenous pressure				
1	Kaolin	353	aut.	CAN
2	Kaolin	403	aut.	CAN
3	Kaolin	473	aut.	CAN
4	A1[b]	353	aut.	A1 (no products)
5	A1	403	aut.	A1–CAN
6	A1	473	aut.	Can–Corundum
7	Zeolite A	353	aut.	CAN
8	Zeolite A	403	aut.	CAN
9	Zeolite A	473	aut.	CAN
(b) High temperature syntheses at elevated pressures				
10	Kaolin[c]	573	0.010	SOD–CAN
11	Kaolin	773	0.015	CAN–(SOD)
12	A1	573	0.010	CAN–(SOD)
13	A1	773	0.015	CAN–(SOD)
14	Zeolite A	573	0.010	SOD–(CAN)
15	Zeolite A	648	0.010	SOD
16	Zeolite A	673	0.010	CAN–(SOD)
17	Zeolite A	773	0.015	CAN

[a] SOD: nitrate sodalite: CAN: nitrate cancrinite; minor phase in brackets.
[b] A1: $2SiO_2 + \gamma Al_2O_3$, sintered at 1673 K.
[c] Sintered at 1673 K for 2 h.

Table 2
Crystallographic data and experimental conditions for the structure refinement of nitrate sodalite $Nag[AlSiO_4]_6(NO_3)_2$

Crystal size and shape	0.10 mm, rhombendodecahedral
Data collection:	
Mo Kα radiation (graphite monochromator)	
Temperature	295 K
Cell parameters calculated from 25 reflections in the 2Θ-range of 4–6°	$a_0 = 8.978(1)$ Å
Number of reflections	8805
4190 reflections in the 2Θ-range and range of reciprocal space	$4° \leq 2\Theta \leq 60°$ $-17 \leq h \leq 17$ $-17 \leq k \leq 17$ $-7 \leq l \leq 7$
4615 reflections in the 2Θ-range and rang of reciprocal space	$60° \leq 2\Theta \leq 120°$ $0 \leq h \leq 25$ $0 \leq k \leq 25$ $-10 \leq l \leq 10$
Number of reflections after data reduction	508 [$I < 3\ \alpha(I)$]
Internal R-value	2.3%
R-value (unweighted)	2.9%
R-value (weighted)	2.0%
Number of refined parameters	42

plitude in a rotating frame. 20 scans were accumulated with a delay between scans up to 10 s. For identification of spinning sidebands, the rotation rate was varied between 2800 and 4500 Hz. The chemical shift has been related to solid NaCl = 0 ppm.

3. Results

3.1. Hydrothermal synthesis

The results of hydrothermal syntheses are summarized in Table 1(a) (synthesis at low temperatures) as well as Table 1(b) (synthesis at high temperatures and pressures). Under the mild reaction conditions only nitrate intercalated cancrinite, but no sodalites, could be observed in every case. This result is consistent with earlier investigations on nitrate intercalated cancrinite crystallization [21–23]. In contrast, at high temperatures and pressures nitrate intercalated sodalite $Na_8[AlSiO_4]_6(NO_3)_2$ could be synthesized together with cancrinite, but exclusively at 648 K and 0.1 GPa as a single phase product. The crystal quality of the sodalites is highly dependent on the nature of the Si–Al source in the starting substances. The best crystals were obtained using Zeolite A (experiment No. 15, Table 1(b)).

The X-ray powder data for nitrate sodalite and nitrate cancrinite are already known from the literature [13,24]. The cubic cell parameter $a_0 = 8.978(1)$ Å for the sodalite single crystals used for further structural calculations was refined on the basis of X-ray powder diffraction, as well as from diffractometer data. For nitrate cancrinite, the lattice parameters $a_0 = 12.649(4)$ Å and $c_0 = 5.192(1)$ Å were refined from X-ray powder data. For both synthesized phases, the sodalites and the cancrinites, the cell parameters are very sensitive to slight deviations of the degree of filling of the porous structure with the guest species. The overall composition of the synthesized phases can be described as nearly ideal and water-free for the sodalites: $Na_8[AlSiO_4]_6(NO_3)_2$ and $Na_{7.7}[AlSiO_4]_6(NO_3)_{1.7} \cdot 2.2H_2O$ for the cancrinites according to thermogravimetric analysis.

IR spectroscopic results, given in Fig. 1, clearly indicate the enclathration of NO_3^- within the sodalite cages exclusively (absorption band at 1380 cm^{-1}; Fig. 1(a)).

In the IR spectrum of cancrinite, a band split for the nitrate absorbtion can be seen (1380 and 1410 cm^{-1}). In contrast to the sodalite, hydroxyl groups (sharp absorption bands at 3520 and 3600 cm^{-1}) as well as water molecules (broad band from 3100–3600 cm^{-1} and sharp absorption at 1650 cm^{-1}) are intercalated into the more open cancrinite channel-structure [23,24] (Fig. 1(c)). The structural arrangement of these additional templates, together with the nitrate anions in the hexagonal channel of the cancrinite framework, are responsible for the band-splitting of the intercalated nitrate. Fig. 1(b) shows the spectrum of a sodalite–cancrinite mixture (product No. 10, Table 1(b)).

The result of the MAS NMR investigation is given in Figs. 2(a)–2(b). Whereas the ^{29}Si MAS NMR spectra of both phases are already known from the literature [13,24], additional spectra of the ^{23}Na nucleus have not been performed until now. The former spectra confirm the alternating Si,Al ordering of the framework of nitrate sodalite according to a single peak at $\delta iso = -86.7$ ppm for Si(4Al) units [13] as well

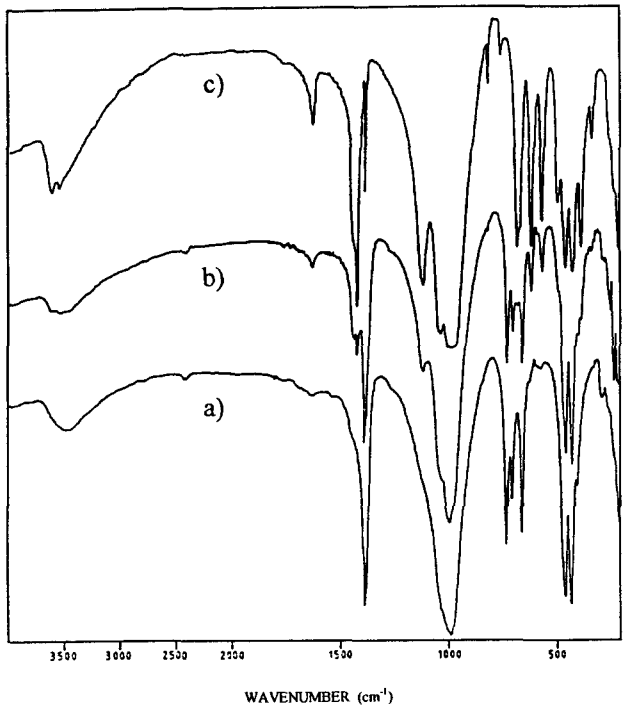

Fig. 1. IR spectra of selected products: (a) nitrate sodalite (No. 15, Table 1(b)); (b) nitrate sodalite + nitrate cancrinite (No. 10, Table 1(b)); (c) nitrate cancrinite (No. 17, Table 1(b)).

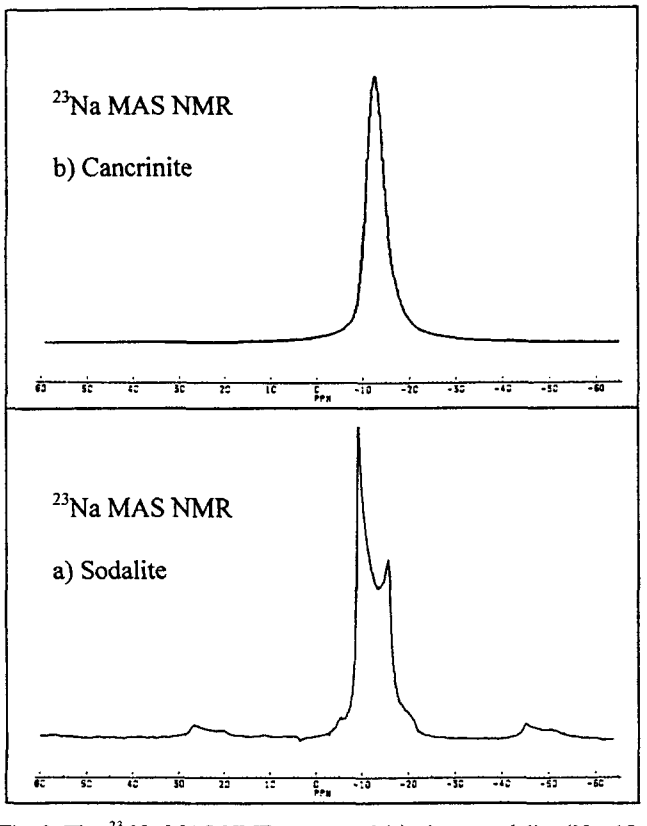

Fig. 2. The ^{23} Na MAS NMR spectra of (a) nitrate sodalite (No. 15, Table 1(b)) and (b) nitrate cancrinite (No. 3, Table 1(a)).

as for the cancrinites (δiso = −86.6 ppm) [24], indicating a Si/Al ratio of 1.0 for both species. In contrast to ^{29}Si MAS NMR, the ^{23}Na MAS NMR spectra indicate major differences for the chemical environment of the sodium cations in the sodalite structure (Fig. 2(a)) compared with the cancrinite structure (Fig. 2(b)). According to the 3/2 spin, the ^{23}Na nuclei possess a quadrupole moment and interact with the local electric field gradients, generating specific powder pattern lineshapes. The width of lineshape and the high-field shift of the centre of gravity from the isotropic chemical shift position is proportional to the square of the quadrupole interaction constant [25]. The ^{23}Na MAS NMR spectrum of nitrate sodalite exhibits the typical quadrupole pattern with two well separated peaks. Minor deviations from the ideal shape of the signal indicate a slight distortion of the axial symmetry of the field gradient. The isotropic chemical shift estimated according to the procedure, given in Ref. [25] is −6.5 ppm. In contrast to this non-spherically symmetric charge distribution around the sodium cations inside the sodalite cages, the ^{23}Na resonance signal exhibits spherical symmetry of the field gradient at the sodium sites, as shown by the MAS NMR spectrum of cancrinite (Fig. 2(b)). This 'increase' in symmetry is responsible for a narrow line in the spectrum, but a slightly unsymmetrical lineshape also suggests quadrupolar line-broadening and results in a location of the chemical shift on the low-field line. The isotropic chemical shift estimated according to the procedure given in Ref. [25] is −12.6 ppm. Structure refinement of nitrate cancrinite is now in progress.

3.2. Structure refinement of nitrate sodalite

Whereas the structure of the aluminosilicate sodalite framework with the tetrahedral arrangement of sodium cations inside the sodalite cages has been known for a long time [26,27], the structural arrangement of the intercalated nitrate is new and interesting, because this trigonal anion breaks the cubic symmetry at the centre of the sodalite cage. From this point of view the arrangement of the nitrate-guests inside the sodalite host-framework should give rise to a high degree of orientational disorder of the enclathrated nitrate anions within the sodalite matrix.

A first refinement of our structure model with nitrogen at the centre of the sodalite cage converged at $R_w = 0.024$. Here, two oxygen atoms were arranged on the position 24i, whereas the remaining third oxygen of the nitrate group was placed on the special position 12f of space group $P\bar{4}3n$. On the basis of this first structure model, the NO_3^- anions reveal a 12-fold orientational disorder, as is shown in Fig. 3.

Despite the goodness of fit between the structural parameters on the basis of this initial model, the

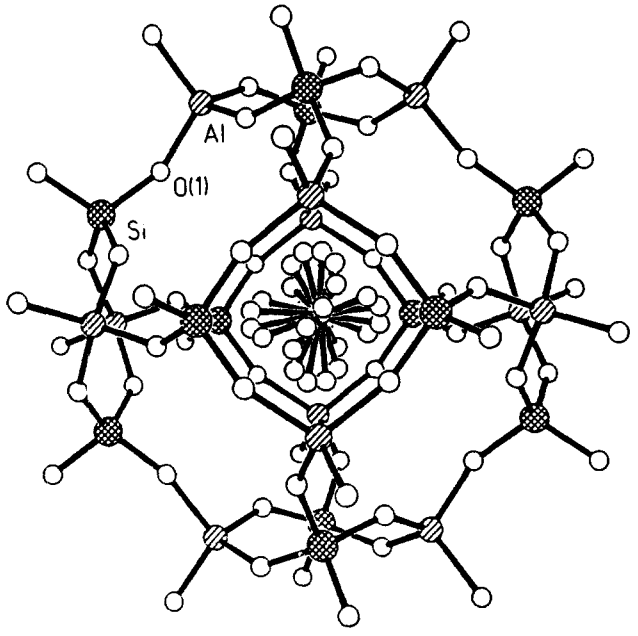

Fig. 3. Model of the positional disorder of the nitrate anion in the sodalite cage (N-atom located at the centre position 0,0,0; not all the O-atoms of the disordered oxoanion and no Na-cations are apparent).

calculated interatomic distances and angles of the intercalated guest anions indicate major deviations compared with the geometry of this group in solid $NaNO_3$ (N–O = 1.24 Å, O–N–O = 120° [19,20]). These distortions are caused by the 12-fold disorder of the NO_3^- anions within the sodalite cages, making a detailed study of the position of one single group impossible.

For a better description of the position of the guest anions within the sodalite cages, we carried out a further refinement using constraints on the bond distances and angles of the nitrate group. Considering the NO_3^- as a 'rigid body' with the regular geometry found in solid $NaNO_3$ [19,20], the real position of the guest anions could be determined.

The final atomic parameters and the isotropic temperature factors of this 'rigid-body' refinement together with all e.s.d.s are included in Table 3. Selected

Table 4
Selected interatomic distances (Å) and angles (deg) of nitrate sodalite

Framework			
Si–O1	1.616(2)	Al–O1	1.736(2)
O1–Si–O1 (2×)	113.6(1)	O1–A1–O1 (2×)	111.7(1)
O1–Si–O1 (4×)	107.5(1)	O1–A1–O1 (4×)	107.5(1)
Si–O1–A1	142.6(1)		
Na1–O1	2.380(2)	Na2–O1	2.313(6)
Na coordination			
Na1–O21	2.518(21)	Na2–O21	3.554(17)
Na1–O23	2.487(19)	Na2–O22	3.341(19)
NO_3^- anion			
N1–O21	1.277(26)	O21–N1–O22	119.8(1.7)
N1–O22	1.277(28)	O21–N1–O23	119.8(1.9)
N1–O23	1.277(19)	O22–N1–O23	119.6(1.9)

interatomic distances and bond angles are summarized in Table 4. As known from sodalites with other guest anions [27,28], as well as from ^{29}Si MAS NMR [13,24], the framework of nitrate sodalite consists of completely ordered AlO_4 and SiO_4 tetrahedra, with a Si–O–Al bonding angle of 142.6(1)° and a Si/Al ratio of 1.0 (see Table 4). Two independent sodium sites could be detected, but all placed on the 8e position of space group $P\bar{4}3n$, i.e. located on the body diagonals, close to the six membered rings of AlO_4 and SiO_4 tetrahedra of the framework. The slight deficit of sodium ions (7.9 Na), given from the refinement of the occupancy of the positions, is in agreement with a total cage filling with nitrate of 95%. This indicates slight deviations from the ideal stoichiometry of the investigated crystal, including 8 Na for balancing the negative charge of the framework and the guest anions. This phenomenon, often observed during hydrothermal synthesis in a highly alkaline medium, seems to be a result of kinetic effects, depending on the reaction temperature and the temperature gradient within the autoclaves.

The position of the nitrate within the tetrahedral arrangement of the sodium cations in the sodalite cage is shown in Figs. 4(a)–4(b). Considering the observed

Table 3
Fractional coordinates and equivalent displacement parameters of nitrate sodalite (e.s.d.s are given in parentheses)

Atom	Site	Occupancy	x	y	z	U_{eq} [a]
Si	6 d	1.0	0.250	0.000	0.500	0.0070(4)
Al	6 c	1.0	0.250	0.500	0.000	0.0068(5)
O1	24 i	1.0	0.115(2)	0.4484(1)	0.1514(2)	0.0122(5)
Na1	8 e	0.7769(1)	0.6911(3)	0.6911(3)	0.6911(3)	0.0234(4)
Na2	8 e	0.2093(1)	0.7040(12)	0.7040(12)	0.7040(12)	0.034(2)
N	24 i	0.0800(5)	0.494(2)	0.513(2)	0.509(2)	0.039(3)[b]
O21	24 i	0.0800(5)	0.377(2)	0.449(2)	0.459(2)	0.033(3)[b]
O22	24 i	0.050(3)	0.572(2)	0.448(2)	0.609(2)	0.050(3)[b]
O23	24 i	0.0800(5)	0.519(2)	0.650(1)	0.478(2)	0.018(3)[b]

[a] $U_{eq} = (1/24\pi^2)\ \Sigma_i\ \Sigma_j\ b_{ij}a_i^*a_j^*a_ia_j$. [b] Isotropic refinement.

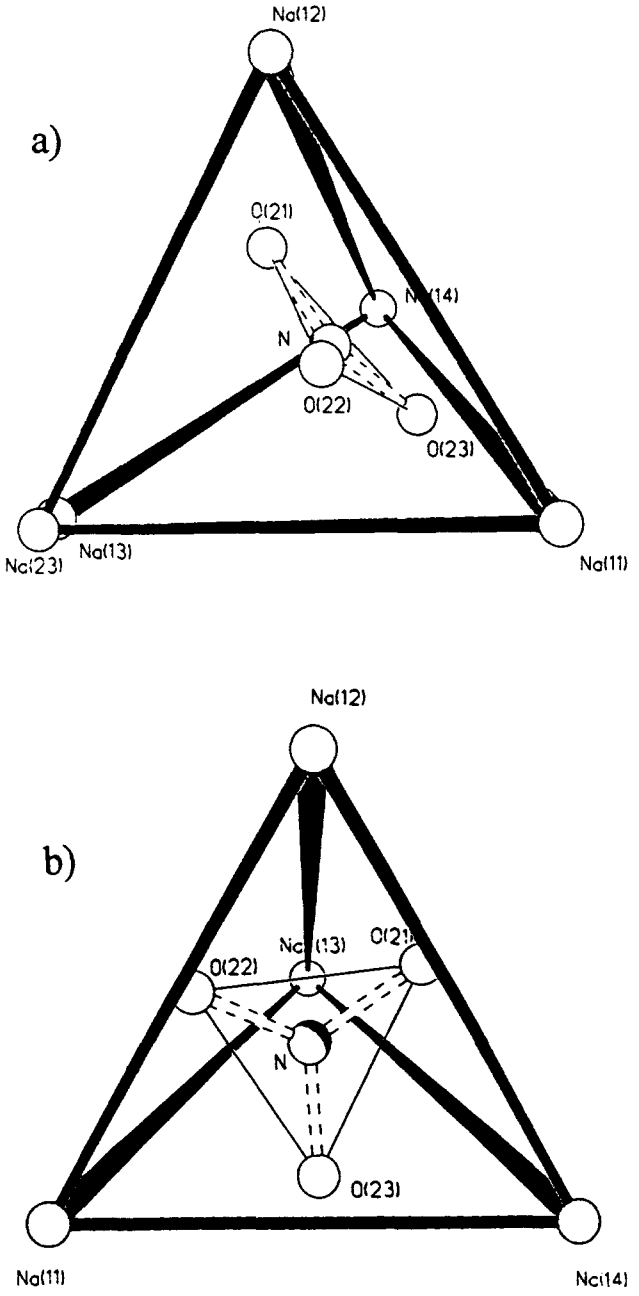

Fig. 4. The position of the nitrate group within the tetrahedral arrangement of the sodium cations of nitrate sodalite. (a) The three-fold axis Na(23)–N is in the paper-plane (a symmetry equivalent Na(13) position is drawn for clarity (but not realized) here near the real Na(23) cation to illustrate the split positions of the Na sites. (b) The same arrangement after a 120° vertical rotation (the split positions of the sodium cations are not drawn).

arrangement under static conditions, one out of the four Na cations exhibits a somewhat shorter Na–O distance to the oxygen atoms of the nitrate. As already described above, the ^{23}Na MAS NMR investigation has been performed to check the static- or dynamic-character of the observed different sodium positions. From the typical quadrupole pattern of the spectrum in Fig. 3(a), dynamic averaging of the orientational disorder of the nitrate anions in the sodalite cages can be suggested. Further experiments, e.g. elastic and inelastic neutron scattering, are necessary to clarify the transition from static to dynamic orientation of the guest species in nitrate sodalite.

Another interesting structural property of nitrate sodalite should be mentioned here. From our DTA and calorimetric investigation [13], a reversible structural phase transition has been obtained at a transition temperature of $T_{tr} = 920$ K. This transition indicates special host–guest interactions owing to the dynamics of the enclosed NO_3^- as well as the sodium cations. Structure refinement of the high-temperature form of nitrate sodalite is currently in progress.

Acknowledgements

The authors are gratefully indebted to Professor Dr. W. Hoffmann (Münster) for valuable discussions and to Dr. G. Engelhardt (Stuttgart) for the performance and discussion of the MAS NMR.

References

[1] H. Saalfeld and W. Depmeier, *Krist. Tech., 7* (1972) 229.
[2] Ch. Baerlocher and W.M. Meier, *Helv. Chim. Acta, 52* (1969) 1853.
[3] R.M. Barrer and J.F. Cole, *J. Chem. Soc. A*, (1970) 1516.
[4] F. Hund, *Z. Anorg. Allg. Chem., 509* (1984) 225.
[5] J. Felsche and S. Luger, *Thermochim. Acta, 113* (1987) 35.
[6] M. Fleet, *Acta Crystallogr. Sect. C:, 45* (1988) 843.
[7] J.-C. Buhl, G. Engelhardt and J. Felsche, *Zeolites, 9* (1989) 40.
[8] J.-C. Buhl and S. Luger, *Thermochim. Acta, 168* (1990) 253.
[9] T. Veit, J.-C. Buhl and W. Hoffmann, *Catal. Today, 8* (1991) 405.
[10] J.-C. Buhl, *J. Cryst. Growth, 108* (1991) 143.
[11] J.-C. Buhl, *J. Solid State Chem., 94* (1991) 19.
[12] J.-C. Buhl and J. Löns, *J. Solid State Chem., 112* (1994) 243.
[13] J.-C. Buhl, *Thermochim. Acta, 189* (1991) 75.
[14] M. Hesse, H. Meier and B. Zeeh, *Spektroskopische Methoden in der organischen Chemie*, Thieme, Stuttgart, 1984.
[15] D. Taylor, *Miner. Mag., 38* (1972) 593.
[16] *International Tables For X-Ray Crystallography*, Vol. 4, Kynoch Press, Birmingham, 1974.
[17] G.M. Sheldrick, SHELX 76, *Programm for Crystal Structure Determination*, Cambridge ,1976.
[18] J.-C. Buhl, *Habilitation Thesis*, University of Münster, Münster, 1991.
[19] S. Göttlicher and C.D. Knöchel, *Z. Kristallogr., 148* (1978) 101.
[20] S. Göttlicher and C.D. Knöchel, Acta Crystallogr. B36 (1980) 1271.
[21] R.M. Barrer, J.F. Cole and H. Villiger, *J. Chem. Soc. A*, (1970) 1523.
[22] F. Hund, *Z. Anorg. Allg. Chem., 511* (1984) 153.
[23] U. Taphorn, *Diploma Thesis*, University of Münster, Münster, 1991.

[24] U. Taphorn, J.-C. Buhl, J. Löns and W. Hoffmann, *Ber. Dtsch. Miner. Ges. Beih. Eur. J. Miner.*, *3* (1) (1991) 265.
[25] E. Kundla, A. Samoson and E. Lippmaa, *Chem. Phys. Lett.*, *83* (1981) 229.
[26] L. Pauling, *Z. Kristallgr.*, *74* (1930) 213.
[27] J. Löns and H. Schulz, *Acta Crystallogr.*, *23* (1967) 434.
[28] P. Kempa, G. Engelhardt, J.-Ch. Buhl, J. Felsche G. Harvey and Ch. Baerlocher, *Zeolites*, *11* (1991) 558.